Supplement of Atmos. Chem. Phys., 25, 11157–11182, 2025
https://doi.org/10.5194/acp-25-11157-2025-supplement

Atmospheric Chemistry and Physics
Open Access
EGU

Supplement of

Adiabatic and radiative cooling are both important causes of aerosol activation in simulated fog events in Europe

Pratapaditya Ghosh et al.

Correspondence to: Hamish Gordon (gordon@cmu.edu)

Table S1: Normalized Mean Bias Factor (NMBF) for N_d for different simulations (for the 500 m model) of all fog cases.

Fog Case	**Def-ARG**	**AD**	**AD-RAD**	**AD-RAD-SED**	**AD-RAD-INV**	**AD-RAD-DCAT**
Nov 15 02:30	0.74	1.97	2.67	0.67	2.49	0.29
Nov 16 01:10	-9.01	-0.06	0.16	-1.43	0.16	-1.90
Nov 16 16:00	-3.31	-0.05	0.03	-1.10	0.01	-1.63
Nov 18 01:30	0.08	0.34	2.55	0.82	1.60	0.95
Nov 19 22:00	-5.18	-0.96	0.35	-0.20	0.08	-0.14
Nov 21 23:50	-7.08	-0.64	0.92	0.15	0.51	0.27
Nov 22 20:50	0.68	2.23	4.78	2.91	2.69	3.17
Nov 23 03:25	-0.08	0.02	0.16	-0.67	-0.23	-0.89
Nov 24 06:20	0.06	-0.17	1.18	-0.51	0.84	-0.55
Nov 24 16:10	-0.15	2.05	4.52	2.42	4.56	1.12
Nov 25 21:40	-4.09	-1.52	0.31	-0.27	0.13	-0.14

Table S2: Normalized Mean Error Factor (NMEF) for N_d for different simulations (for the 500 m model) of all fog cases.

Fog Case	**Def-ARG**	**AD**	**AD-RAD**	**AD-RAD-SED**	**AD-RAD-INV**	**AD-RAD-DCAT**
Nov 15 02:30	1.02	2.02	2.72	0.87	2.54	0.87
Nov 16 01:10	9.25	0.33	0.37	1.75	0.36	2.24
Nov 16 16:00	3.45	0.34	0.35	1.25	0.32	1.81
Nov 18 01:30	0.70	0.89	2.55	0.98	1.60	1.07
Nov 19 22:00	5.83	1.42	0.99	0.81	0.77	0.77
Nov 21 23:50	8.07	1.24	1.03	0.81	0.91	0.81
Nov 22 20:50	0.89	2.23	4.78	2.91	2.69	3.17
Nov 23 03:25	0.56	0.56	0.60	1.00	0.70	1.26
Nov 24 06:20	0.71	0.64	1.61	0.72	1.27	0.73
Nov 24 16:10	2.10	2.23	4.52	2.42	4.56	1.20
Nov 25 21:40	4.46	1.78	0.71	0.76	0.80	0.72

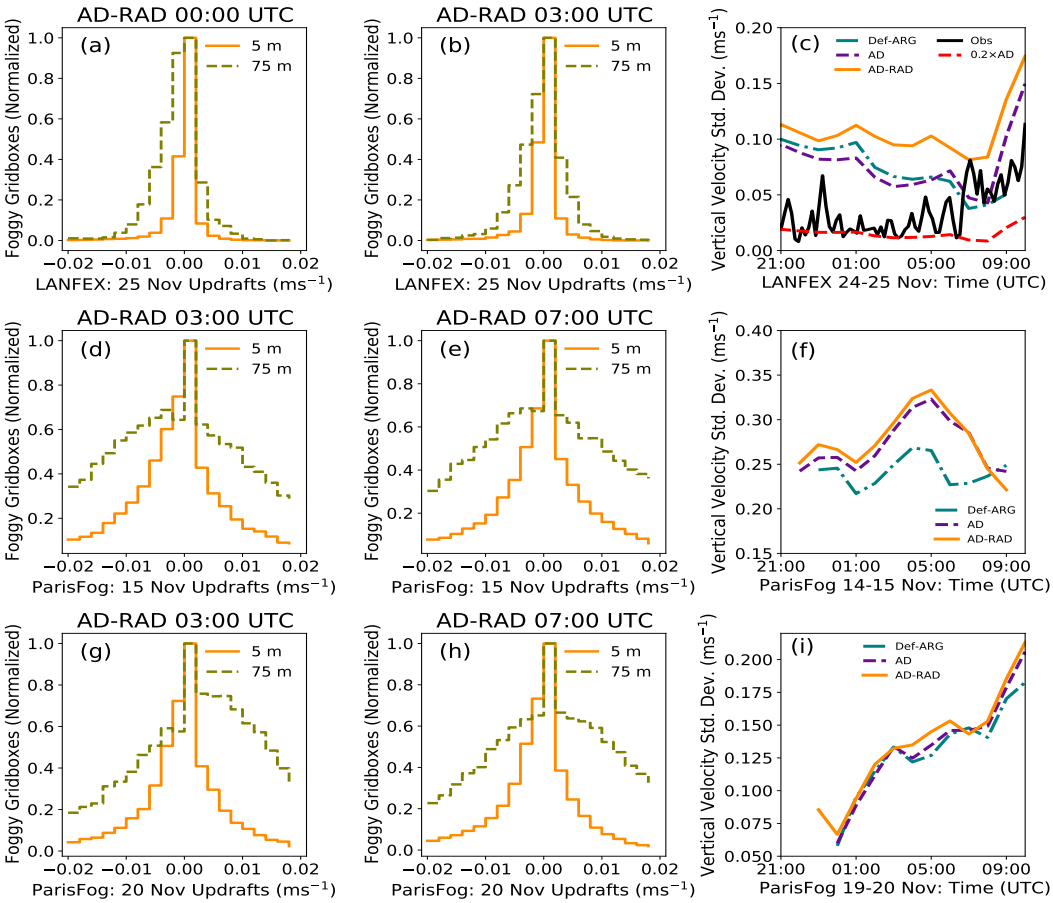

Figure S1: Histogram of resolved updrafts (left and middle panel) at the 5 m and 75 m altitude for LANFEX and two ParisFog cases are shown here from the AD-RAD simulation. The right panel shows the simulated standard deviation (σ_w) of unresolved sub-grid updrafts (the square root of the diagnosed unresolved subgrid updraft variance) from Def-ARG, AD and AD-RAD simulations (and observations for the LANFEX case) for the same fog cases at the surface. In subfigure (c), we demonstrate that the width of the updrafts is overestimated by a factor of 5 in our simulations. These results motivate the choice of prefactor 'c' in the companion paper. These results are from the foggy gridboxes only.

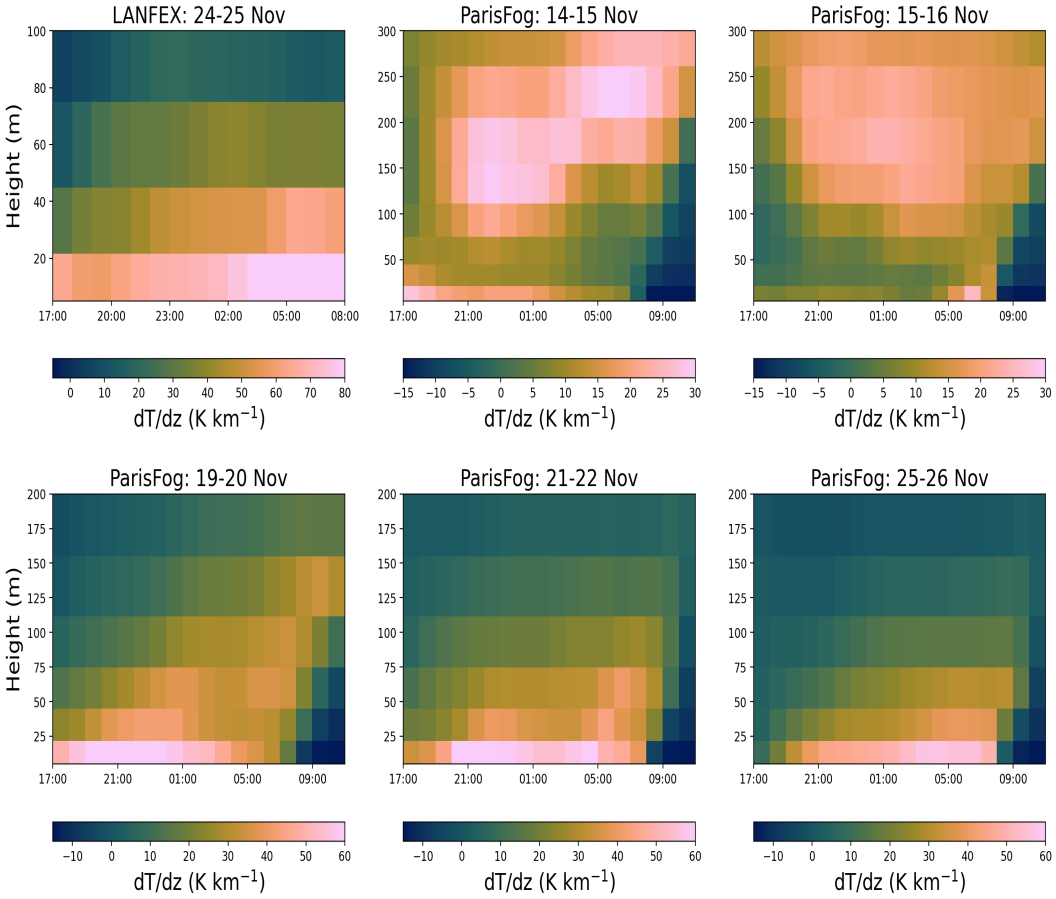

Figure S2: Vertical profile of change in temperature with altitude in simulation Def-ARG, derived from the 500 m resolution model. The difference in temperature between two adjacent model levels in divided by the distance between the midpoints. Note the different y axis scales between different subfigures.

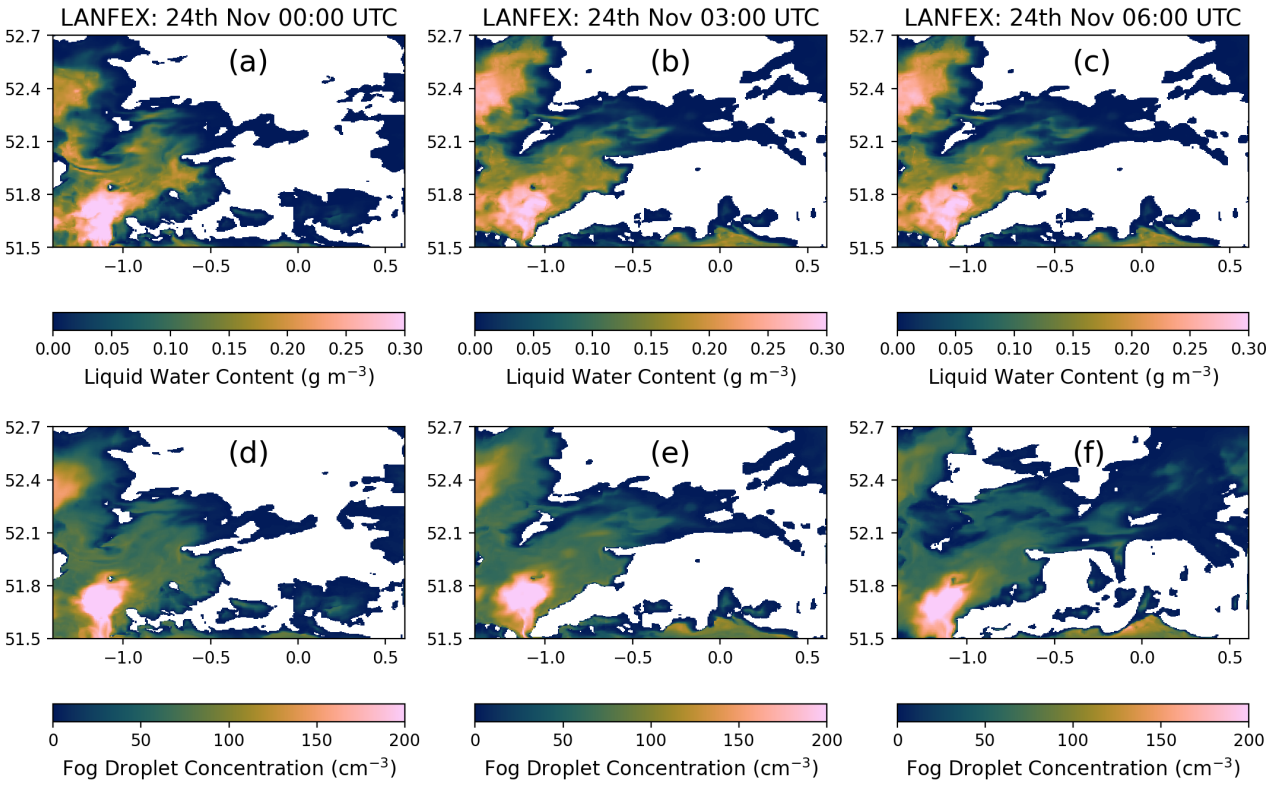

Figure S3: Spatial variation of grid-average N_d and LWC on 24 November during the LANFEX field campaign for different times (UTC). We show these properties near the surface in our 500 m model from the AD-RAD simulation.

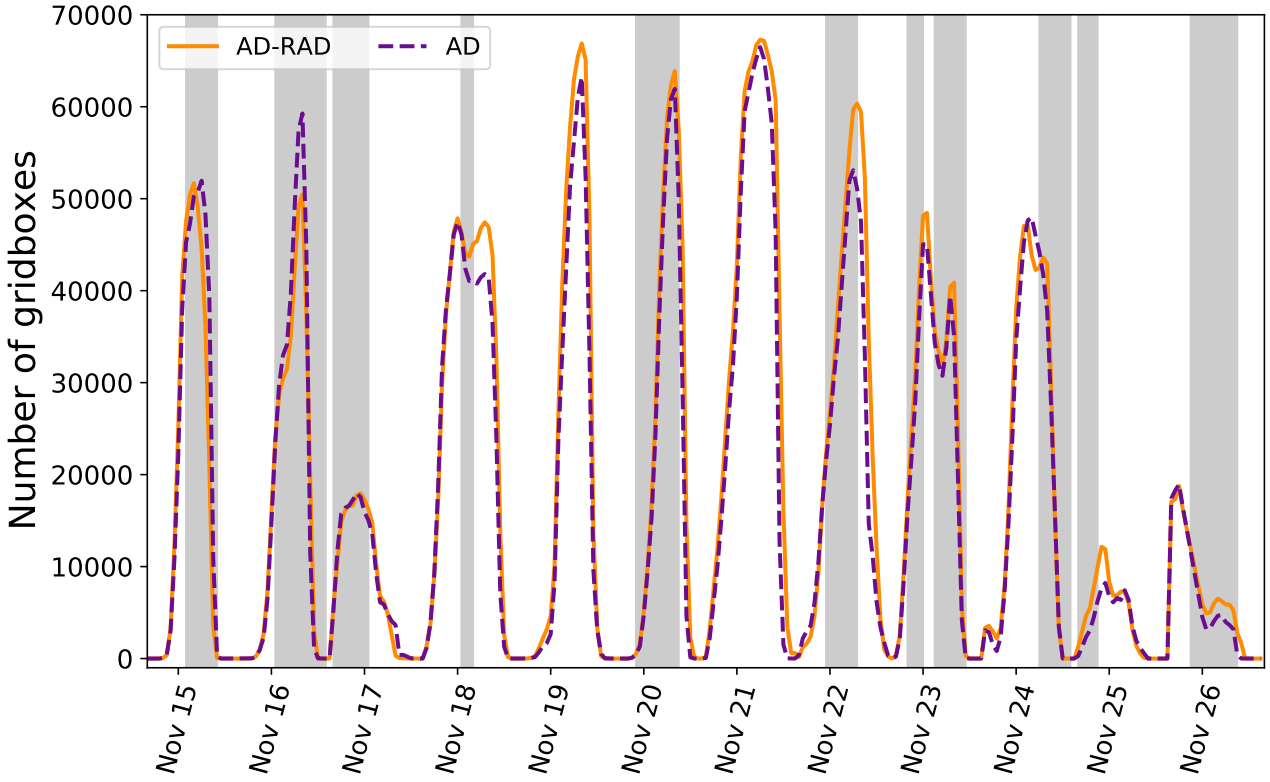

Figure S4: Timeseries of number of foggy gridboxes at the surface of the 500 m model from simulations AD and AD-RAD during different ParisFog cases.

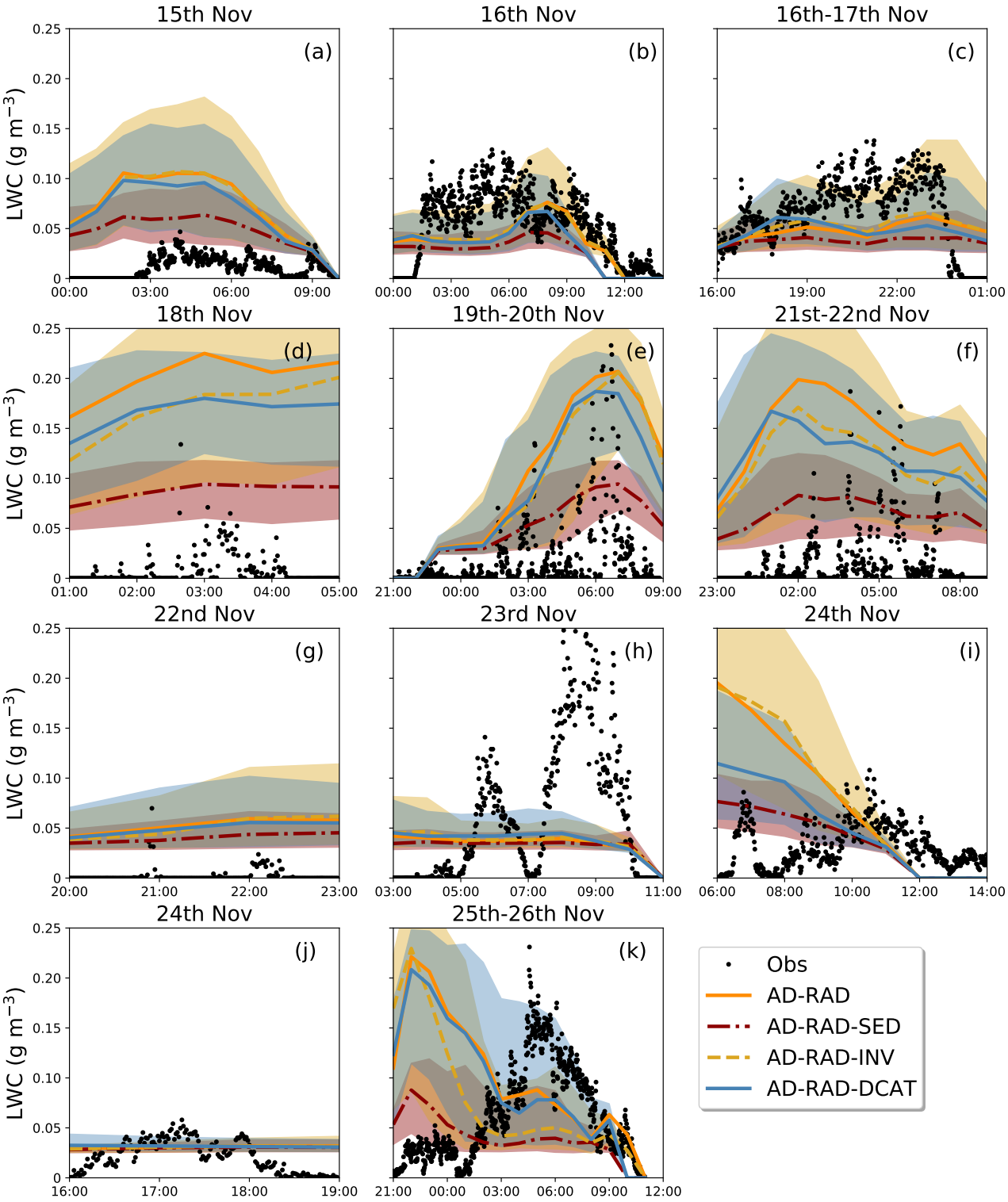

Figure S5: Variation of simulated and observed liquid water content as a function of time for different fog events. The results of the 500 m model near the surface from the simulations AD-RAD-SED, AD-RAD-INV, and AD-RAD-DCAT are compared with observations at the SIRTA observatory (UTC time). The solid and dashed lines represent the median values, and the shaded regions represent the interquartile ranges over the foggy gridboxes. We also show the median N_d from AD-RAD in orange solid lines for comparison.

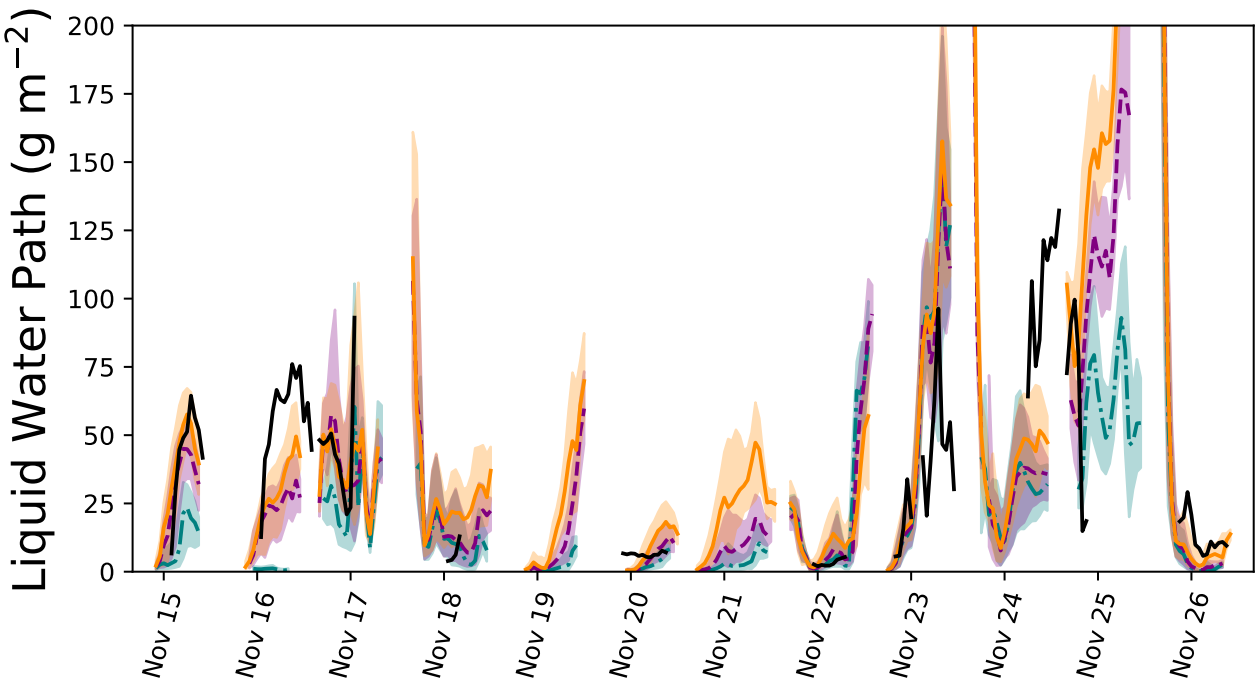

Figure S6: Time series of Liquid Water Path (in the 500 m model) during the ParisFog cases with and without radiative cooling included in aerosol activation for simulations Def-ARG, AD and AD-RAD.

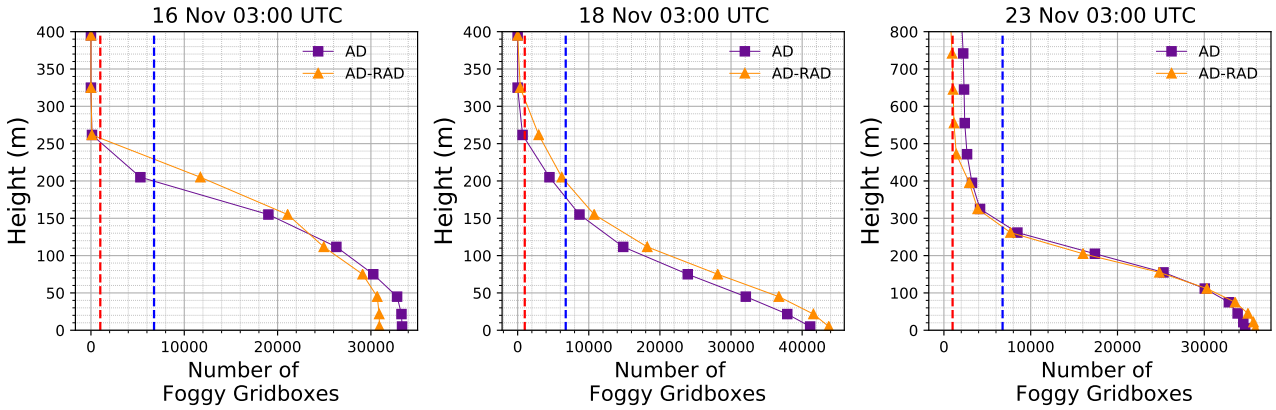

Figure S7: Vertical profiles of number of foggy gridboxes for the 16$^{\text{th}}$, 18$^{\text{th}}$, and 23$^{\text{rd}}$ November ParisFog cases (at 03:00 UTC) for simulations AD and AD-RAD. Red and blue dotted vertical lines represent 1000 (our threshold) and 6760 (10% of 260 x 260 gridboxes used in the analysis) foggy gridboxes, respectively. The 'Height' axis is different for the 23 November fog case.

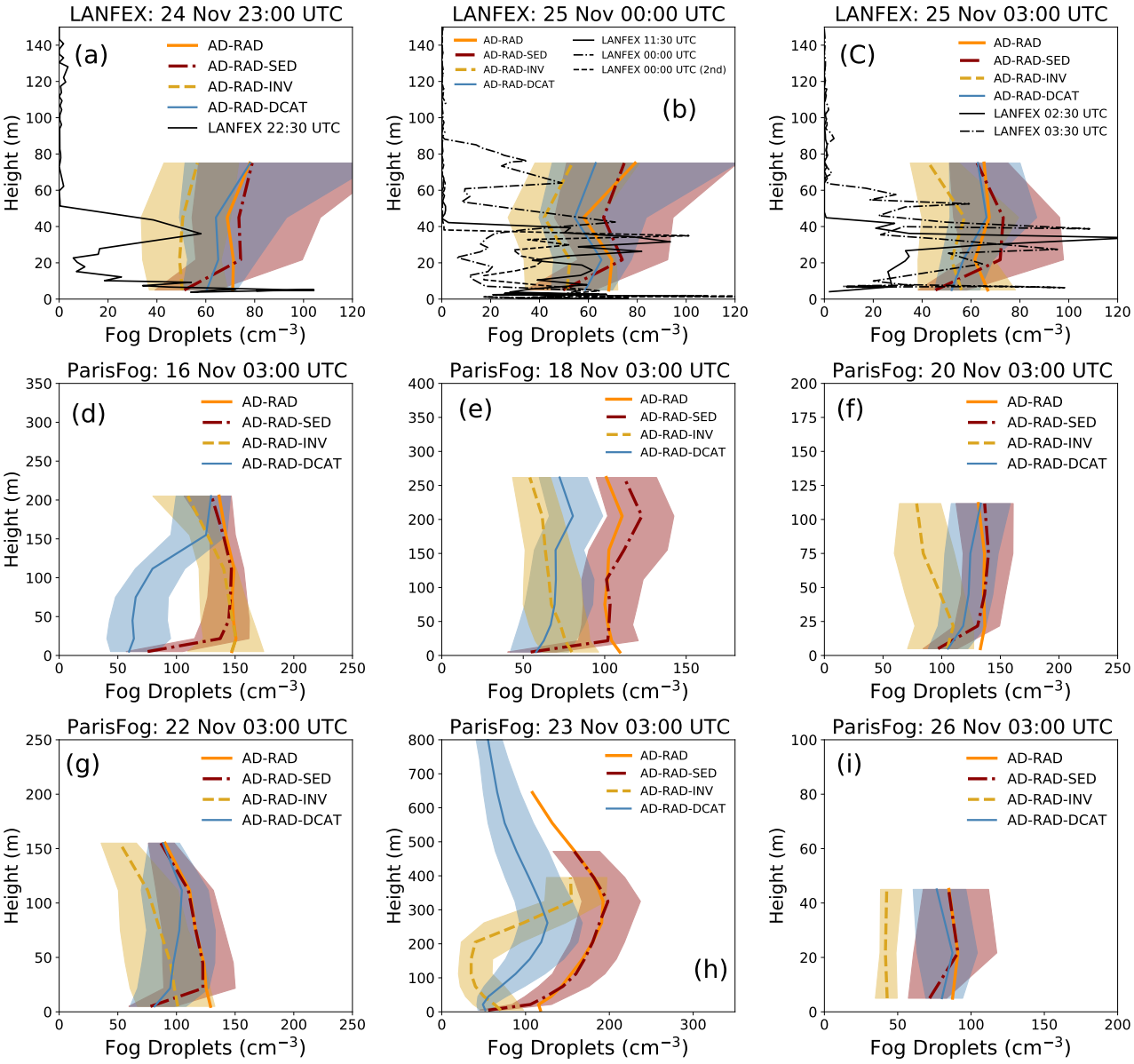

Figure S8: Vertical Profiles of N_d from the LANFEX case study and different days of the ParisFog case study. The median and interquartile range from the 500 m model for AD-RAD-SED, AD-RAD-INV, and AD-RAD-DCAT simulations are shown here. The median from AD-RAD is also plotted for comparison. Observations during LANFEX are from the fog monitor kept in the tethered balloon.

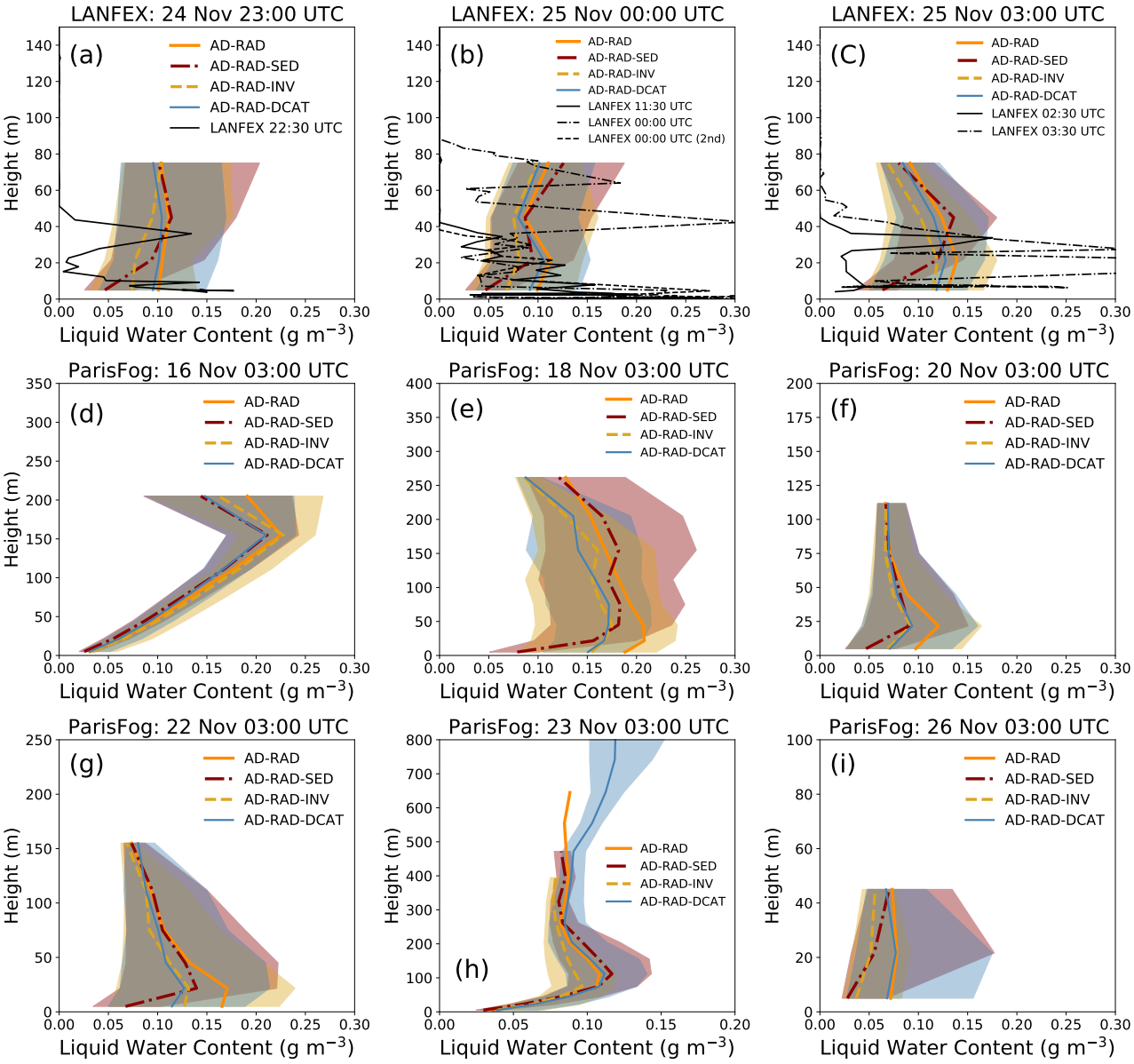

Figure S9: Vertical Profiles of LWC from the LANFEX case study and different days of the ParisFog case study. The median and interquartile range from the 500 m model for AD-RAD-SED, AD-RAD-INV, and AD-RAD-DCAT simulations are shown here. The median from AD-RAD is also plotted for comparison. Observations during LANFEX are from the fog monitor kept in the tethered balloon.

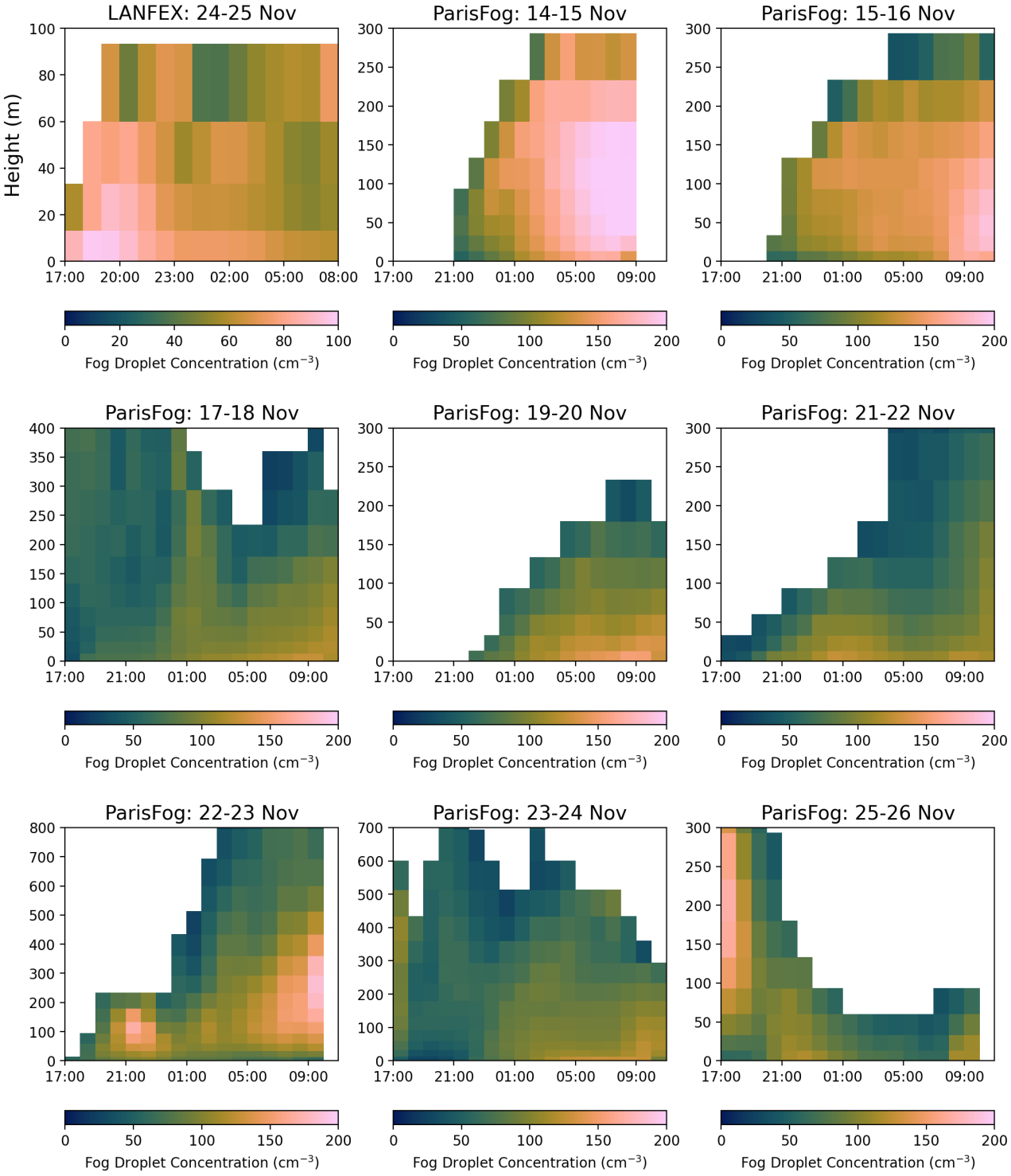

Figure S10: Vertical profile of N_d in our 500 m AD-RAD simulation, as a function of time (UTC) from the LANFEX case and different ParisFog cases. The mean in-fog N_d of all foggy gridboxes (at the surface and their vertical column following the main text) are taken.

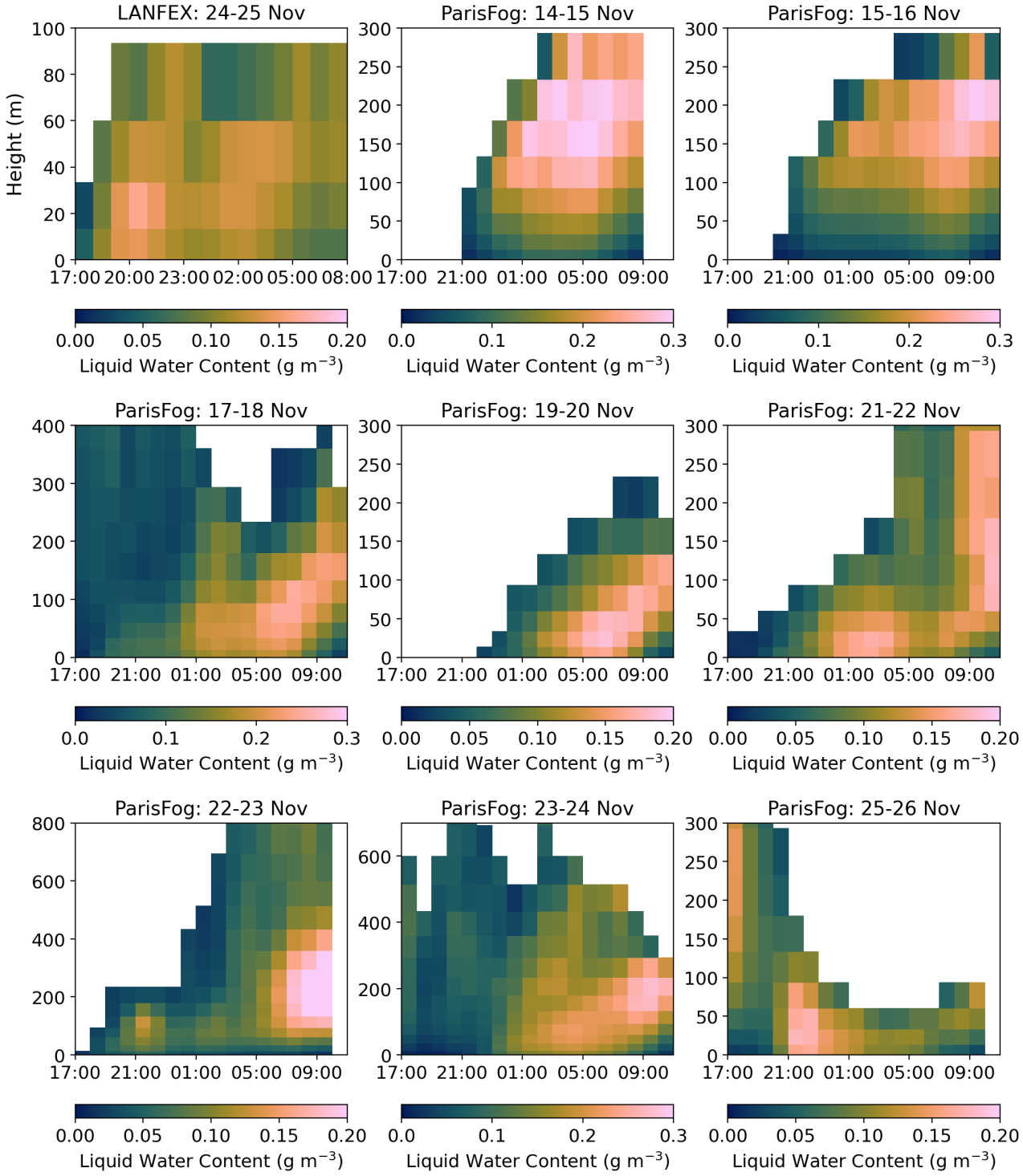

Figure S11: Vertical profile of LWC in our 500 m AD-RAD simulation, as a function of time (UTC) from the LANFEX case and different ParisFog cases. The mean in-fog LWC of all foggy gridboxes (at the surface and their vertical column following the main text) are taken.